Ice stream basal conditions from block-wise surface data inversion and simple regression models of ice stream flow: Application to Bindschadler Ice Stream

O. V. Sergienko,[1] R. A. Bindschadler,[2] P. L. Vornberger,[3] and D. R. MacAyeal[4]

Received 20 February 2008; revised 20 June 2008; accepted 3 September 2008; published 4 December 2008.

[1] Widespread basal conditions controlling ice stream flows are still beyond the scope of direct observation, thus knowledge of their magnitudes and variabilities comes from inversion of surface measurements: ice velocities, surface elevations, and thicknesses. We present a new approach to implement a widely accepted inverse method on regular (10 × 10 km) blocks, smaller than the whole domain, to enhance the spatial resolution of calculated basal conditions. Inverted basal friction coefficients and calculated shear stress have sharp transitions and large variations in small areas. Overall, the obtained basal shear stress is very small in regions of fast flowing ice. The results of the inversion, along with the surface variables, are used to construct two simple regression models of Bindschadler Ice Stream (former Ice Stream D) that reproduce 96% of observed velocity variations. While highly idealized, these regression models are sufficiently informative to be considered as parameterizations for ice stream flow in large-scale ice sheet models which lack the spatial and temporal resolution necessary to simulate ice stream dynamics in detail.

Citation: Sergienko, O. V., R. A. Bindschadler, P. L. Vornberger, and D. R. MacAyeal (2008), Ice stream basal conditions from block-wise surface data inversion and simple regression models of ice stream flow: Application to Bindschadler Ice Stream, *J. Geophys. Res.*, *113*, F04010, doi:10.1029/2008JF001004.

1. Introduction

[2] Since the discovery of Antarctic ice streams [*Rose*, 1979] the long-continued debate about their origin [*Bentley*, 1987] has converged on the conclusion that their fast motion is caused by low basal drag, possibly because of a layer of deforming basal sediment [*Alley et al.*, 1987; *Blankenship et al.*, 1986; *Tulaczyk et al.*, 2000; *Peters et al.*, 2006]. The direct measurement of this basal drag over large areas is not practical because it requires widespread direct access to the bed. As a consequence, inverse methods applied to surface observations have become the primary method for estimating ice stream bed properties. An application of these methods to the ice stream problem was developed by *MacAyeal* [1992b], and performed in various Antarctic ice stream studies [*MacAyeal*, 1992b; *Vieli and Payne*, 2003; *Joughin et al.*, 2004]. Inversion of surface data collected on Bindschadler Ice Stream (BIS), former Ice Stream D, has been done in the context of a large-scale examination of the Siple Coast ice stream flow regime that feeds the Ross Ice Shelf [*Joughin et al.*, 2004]. In the present study, inversion of BIS surface data follows the same basic methodology, but uses additional surface data and seeks to obtain results on a high spatial resolution using a spatially piece-wise set of small (10 × 10 km) subdomains that cover the BIS in an overlapping manner. The intended benefit of this novel approach is to increase the spatial resolution of derived basal parameters and better account for observed data relative to what is achieved by single, whole ice stream domain inversions.

[3] There are numerous glaciological studies that focus on ice sheet behavior in circumstances where ice streams are peripherally involved but where precise knowledge of the details of ice stream behavior are not essential to the goals of the study. Examples include studies of the large-scale stability or mass balance of West Antarctic Ice Sheet over long periods of the geologic past [*MacAyeal*, 1992a], and the study of changes in the Greenland Ice Sheet where there is large spatial and temporal variability in ice dynamics. Such studies would benefit tremendously from simple, computationally inexpensive parameterizations that could reproduce ice stream flow reasonably well, e.g., to within a well defined accuracy. To explore the feasibility of such a parameterizations of an ice stream, we create regression parameterizations on the basis of the multiple regression analysis of BIS that relates observed ice stream flow to other parameters such as ice thickness, surface elevation and basal roughness that could be derived from surface imagery. These parameterizations appear to be a promising approach

[1]Geology Department, Portland State University, Portland, Oregon, USA.
[2]Hydrospheric and Biospheric Science Laboratory, NASA Goddard Space Flight Center, Greenbelt, Maryland, USA.
[3]Science Applications International Corporation, Beltsville, Maryland, USA.
[4]Department of the Geophysical Sciences, University of Chicago, Chicago, Illinois, USA.

Copyright 2008 by the American Geophysical Union.
0148-0227/08/2008JF001004

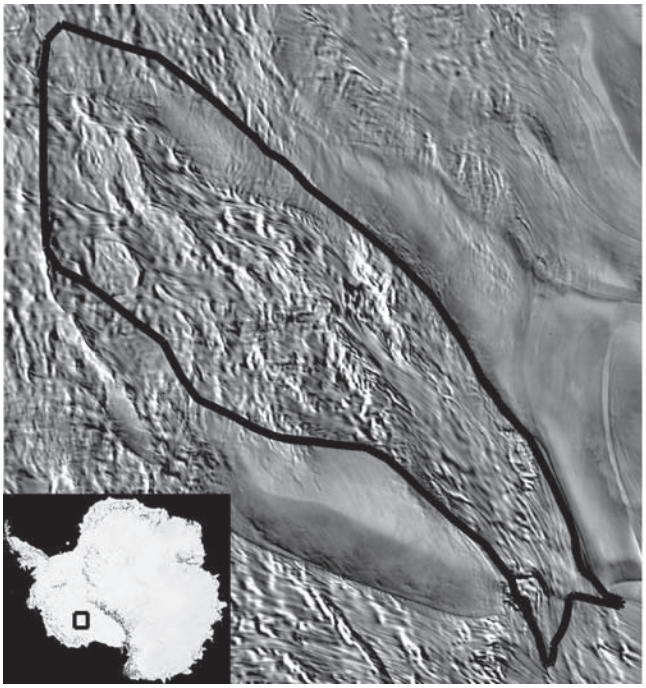

Figure 1. Mosaic of Antarctica (MOA) image of Bindschadler Ice Stream and outline of the study domain. Inset shows map of Antarctica and location of MOA image.

for the treatment of ice streams in nonice-stream-resolving models.

2. Inverse Methodology

[4] Derivation of ice stream basal conditions from surface observations is done in a least squares sense, i.e., the goal is to find ice stream basal conditions such that the sum of squared differences between velocities calculated by using a model with these basal conditions and observed velocities is minimal [*MacAyeal*, 1992b]. Here we briefly describe the steps of this procedure.

[5] The procedure involves several steps: running a forward model of ice stream flow with estimated basal conditions that produces ice stream surface velocities; comparing these model velocities to observed velocities; improving the initial estimate of basal conditions to reduce mismatch between calculated and observed velocities; and repeating these steps until the mismatch between observed and calculated velocities is acceptably small. A parameter that describes this mismatch is usually called a cost function or a performance index, and is an integral of squared differences between calculated and measured velocities. There are a few important cautions involved in this simple, least squares method. First, the inverse problem is one of a class of problems referred to as being "ill posed" [*Isakov*, 1998], thus the derived basal parameters are not unique. This also means that small errors in surface velocities and elevations used as input to the inversion scheme can lead to high amplitude, but otherwise poorly constrained basal friction features in the bed. Inverse methods used to treat this problem can thus, at best, provide only an estimate of possible basal conditions that produce surface velocities similar to observations within discrepancy limits. A possible approach to reducing such uncertainty is to use indirect measurements (e.g., bed roughness [*Bingham and Siegert*, 2007]) to impose additional constraints on inverted basal conditions.

[6] A second caution about the method is that the estimate of basal conditions depends strongly on the physics used in the forward model of the ice stream. Thus, different forward models should produce different basal fields, and better, more physically accurate models should produce the most realistic basal conditions.

2.1. Forward Model

[7] The forward model used here is a two-dimensional, vertically integrated model of ice stream flow developed by *MacAyeal* [1989], i.e., the shelfy stream model described by *Hindmarsh* [2004] and *Schoof* [2006]. The governing equations for horizontal ice velocity components are

$$\frac{\partial}{\partial x}\left[2\nu H\left(2\frac{\partial u}{\partial x}+\frac{\partial v}{\partial y}\right)\right]+\frac{\partial}{\partial y}\left[\nu H\left(\frac{\partial u}{\partial y}+\frac{\partial v}{\partial x}\right)\right]=\rho g H\frac{\partial S}{\partial x}-\tau_u, \tag{1}$$

$$\frac{\partial}{\partial x}\left[\nu H\left(\frac{\partial u}{\partial y}+\frac{\partial v}{\partial x}\right)\right]+\frac{\partial}{\partial y}\left[2\nu H\left(\frac{\partial u}{\partial x}+2\frac{\partial v}{\partial y}\right)\right]=\rho g H\frac{\partial S}{\partial y}-\tau_v, \tag{2}$$

where H is ice thickness, S is surface elevation, $\rho = 910$ kg m^{-3} is ice density, $g = 9.81$ m s^{-2} is the acceleration due to gravity, ν is the effective, strain-rate-dependent ice viscosity representing Glen's flow law given by

$$\nu=\frac{\bar{B}}{2\left[\left(\frac{\partial u}{\partial x}\right)^2+\left(\frac{\partial v}{\partial y}\right)^2+\frac{1}{4}\left(\frac{\partial u}{\partial y}+\frac{\partial v}{\partial x}\right)^2+\frac{\partial u}{\partial x}\frac{\partial v}{\partial y}\right]^{\frac{n-1}{2n}}}, \tag{3}$$

where $\bar{B} = 1.68 \times 10^8$ Pa s$^{1/3}$ is a vertically-averaged ice stiffness parameter, $n = 3$ is the power law flow exponent and τ_u and τ_v are x and y components of the basal shear stress, respectively, defined by

$$\tau_u = -\beta^2 u, \tag{4}$$

$$\tau_v = -\beta^2 v, \tag{5}$$

where β is basal friction coefficient (Pa s m^{-1})$^{\frac{1}{2}}$. It is the parameter sought in the inversion. The square dependence of basal shear $\vec{\tau}$ on β insures that $\vec{\tau}$ always acts in a direction opposite to ice flow without regard to the sign of β. Kinematic boundary conditions are applied on horizontal boundaries enclosing the domain using surface observations to constrain u and v.

[8] The ice stiffness parameter $\bar{B}$ is assumed to be spatially uniform in this study. It is a vertically averaged function of ice temperature, for which direct or indirect observations are not available at this time. Theoretically, it is possible to invert available surface measurements for basal friction coefficient β and the ice stiffness parameter $\bar{B}$ simultaneously, although, in contrast to β that can have wide ranging values because of large variations in surface

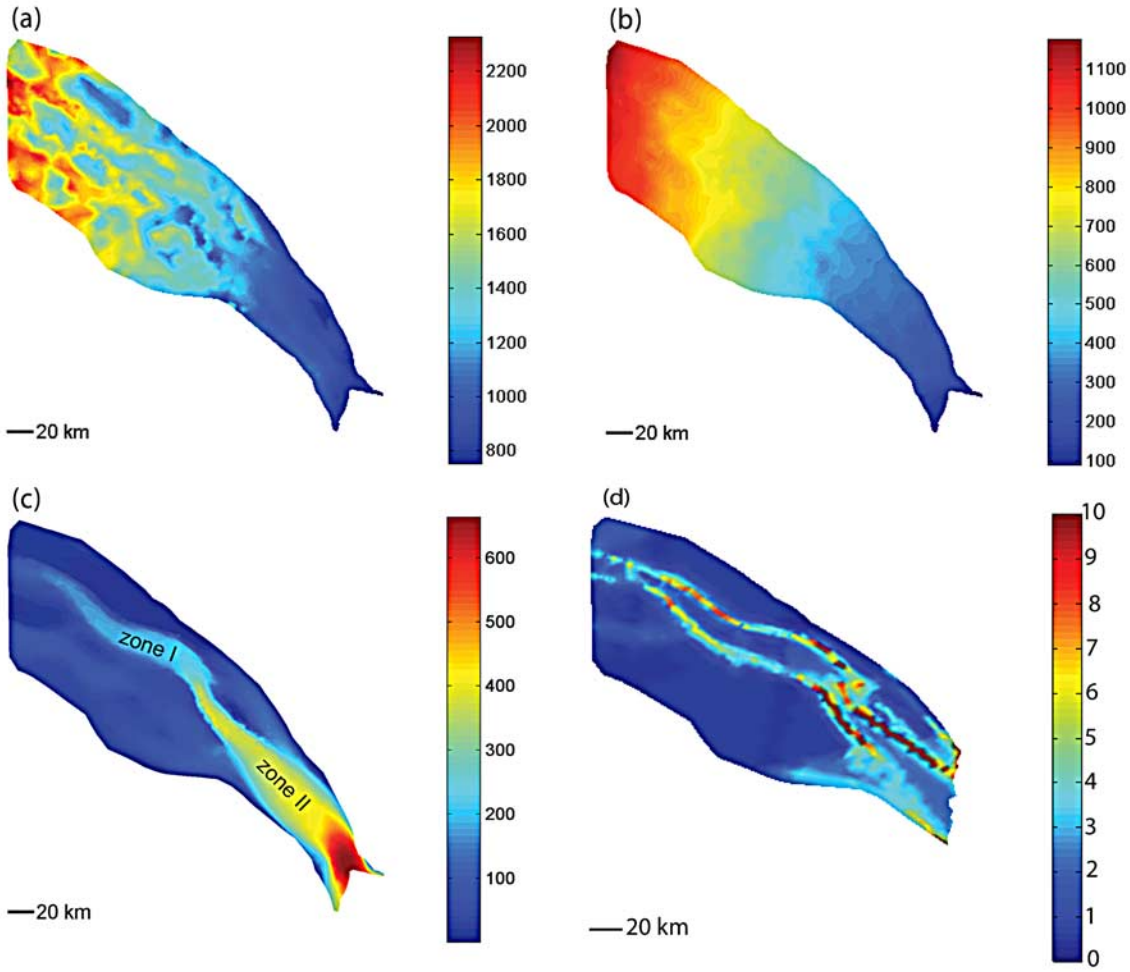

Figure 2. Data used for inversion basal conditions under Bindschadler Ice Stream. (a) Ice thickness (m) derived from CASERTZ observations, (b) surface elevation (m) derived from ICESat observations, (c) ice surface velocity (m a^{-1}) derived from speckle tracking and InSAR observations, and (d) ice velocity errors (m a^{-1}). Zones I and II on Figure 2c denote two distinctive regions of fast flowing ice.

velocities, the possible range of $\bar{B}$ is strictly constrained by ice temperature and ice fabric, and only weakly constrained by surface velocities. Thus, a reliable expectation is that variations in $\bar{B}$ are likely to be large scale and span much of the ice stream with little local change. This means that small-scale variations in surface velocity are predominantly caused by the effects of variable β.

2.2. Input Data: Bindschadler Ice Stream

[9] Satellite imagery of the BIS is displayed in Figure 1. The necessary fields of ice thickness, surface elevation and surface velocities are displayed in Figure 2. We use ice thickness (Figure 2a) measured by the Corridor Aerogeophysics of the South East Ross Transect Zone (CASERTZ) project [*Blankenship et al.*, 2000], surface elevation (Figure 2b) derived from the Ice, Cloud, and Land Elevation Satellite (ICESat) digital elevation model (DEM) [*DiMarzio et al.*, 2007] and surface velocities (Figure 2c) derived from Interferomatetric Satellite Aperture Radar (InSAR) and speckle tracking [*Joughin*, 2002]. CASERTZ ice thickness data were obtained during aerogeophysical surveys at a 5.3 km grid spacing and then interpolated to a 425 m grid using a Gaussian filter and bicubic spline method. Errors of ice thickness measurements over our study domain are ±11 m. ICESat surface elevation and surface velocity data are provided with a 500 m spatial resolution. ICESat errors are order ±20 cm. Ice velocity data have variable errors, over most of the BIS an error of about 5 m a^{-1} (where a is years) applies, but this increases to 30 m a^{-1} along shear boundaries at the lateral edges of the BIS (Figure 2d). Zones I and II in Figure 2c are areas where ice flow is significantly faster than average.

2.3. Block-Wise Inversion Versus Whole Domain Inversion

[10] Two inversion approaches, whole domain and block wise, are compared to assess their relative advantages and disadvantages. Both are based on the methods described above, i.e., running a forward ice stream flow model (equations (1) and (2)) with iteratively improving basal friction coefficients until he the cost function reaches its minimum. As mentioned above, inverted parameters are estimates, rather than exact values. One way to improve accuracy is to impose additional conditions, e.g., specifying an allowed range for the inverted parameters, or demanding a smooth spatial variation of derived parameters. Another

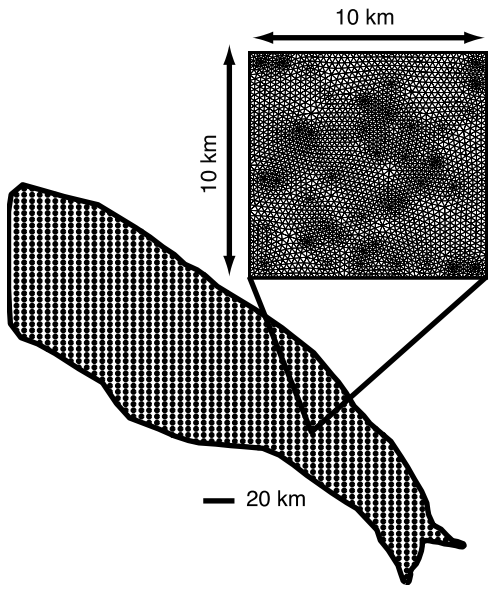

Figure 3. Dots show positions of low left corners of uniform blocks. Dots are spaced in 5 km, that results in overlapping of a uniform block by eight neighboring blocks. Inset shows a uniform block 10 × 10 km used for a block-wise inversion. Finite element mesh has 2577 nods and 4992 elements. Linear spatial resolution is ~250 m.

constraint could be a requirement that the calculated velocity field exactly match the observed velocity field in specific locations. By choosing these locations to be the boundaries of smaller subdomains that cover the full domain of the region of interest, we create a collection of smaller inverse problems (block inversions) where each is similar to the initial inverse problem for the entire domain, i.e., reconstruction of basal conditions from surface observations with prescribed velocities at the boundaries. This collection of smaller inverse problems allows the observed velocity field to be introduced as strong constraints of the whole domain inversion by virtue of the boundary conditions required for each subdomain, and this leads to greater accuracy and higher resolution in the result. Thus, an inverse problem with a constrain to exactly match velocities in specific locations, posed on a whole domain is equivalent to a set of the mutually independent inverse problems on small domains, provided that required locations are on boundaries of small domains.

[11] The advantage of breaking up the full domain into a collection of interlocking block-shaped subdomains that cover the full domain is threefold. First, with additional velocity constraints on the block boundaries, we expect to achieve more realistic estimates of the inverted parameters. Second, isolated areas where it is impossible to find inverted parameters that result in a cost function less than prescribed limit, e.g., areas with poorly known input data, do not affect inverted parameters in other subdomains, as they do in the whole domain inversion. Therefore net misfit of the block-wise inversion is less then the misfit of the whole domain inversion. Third, with the solution within each block separately determined, it is possible to increase the spatial resolution of the overall treatment in a computationally efficient manner. In practice, it is appropriate to limit the horizontal scale of subdomains to maintain consistency with assumptions used in the forward model physics. In our study, the model equations are valid in circumstances where $\frac{H}{L} \ll 1$, where H is the ice thickness and L is the characteristic horizontal length scale. Thus, it is pointless for the horizontal scale of a subdomain to be smaller than the local ice thickness. In our analysis of the BIS, we chose 10 km as the appropriate subdomain size. With high-resolution surface velocity data it is also tempting to perform inversions for basal conditions yielding results on a similar spatial scale. With a study domain spanning 3.2×10^4 km^2 (Figure 1), a 500 m horizontal resolution would require ~130,000 grid points in the numerical representation. Every step of the inversion process requires factorizations of $N \times N$ matrices, where N is number of grid points. Even with rapidly advancing computer technologies it remains a challenge to handle factorizations of such large matrices. The block-wise inversion method allows for this high-resolution solution, but keeps the computational problem (via matrix size) sufficiently small to be tractable.

2.4. Block-Wise Inversion

[12] Block-wise inversion for the basal friction coefficients of BIS was done in the following way. Lower left corners of overlapping rectangular 10 × 10 km blocks were arrayed on a 5 km spacing (Figure 3). Thus, every block, except those adjacent to the domain boundaries, was overlapped by eight neighboring blocks (four covering halves and four covering quarters of the original block). The reason why the blocks are overlapped is that the kinematic boundary condition specified at block boundaries would otherwise prevent meaningful β values at the boundaries. Thus, every location where β is desired must lie inside at least one block. Ambiguity of the derived β associated with multiple inversions of overlapping blocks is handled by a weighted averaging scheme discussed below.

[13] Basal friction coefficients were obtained for each block separately, using the observed velocities at the edges of each block as kinematic boundary conditions. Where blocks overlapped, the resulting basal friction coefficients were averaged with a normalized Gaussian weighting function (Figure 4a). With this weighting function, β at block boundaries do not contribute to the averaging process ($w = 0$ there), and the largest contribution comes from points close to the center of individual blocks. Figures 4b and 4c show a specific example illustrating that the averaging scheme allows for smooth block-to-block transitions.

3. Inverted Basal Conditions Under Bindschadler Ice Stream and Its Stress Balance

[14] The block wise inverted β field is shown in Figure 5a. In contrast to the whole domain inversion (Figure 5b), the block-wise inversion produces greater spatial detail, revealing sharp transitions and large variations in basal friction coefficient in small areas. Overall, the obtained basal friction coefficients are low in regions where observed ice flow is fast (Figures 5 and 2c (zone II)). Basal shear stress calculated with equations (4) and (5) is shown in Figure 6. Zones of fast flowing ice (>100 m a^{-1}) have very low basal friction coefficients (~3×10^4 (Pa s m^{-1})$^{\frac{1}{2}}$), and, consequently, low basal shear τ (~0.3–3 kPa). These zones of fast flowing ice (Figure 2c) can have spatially confined

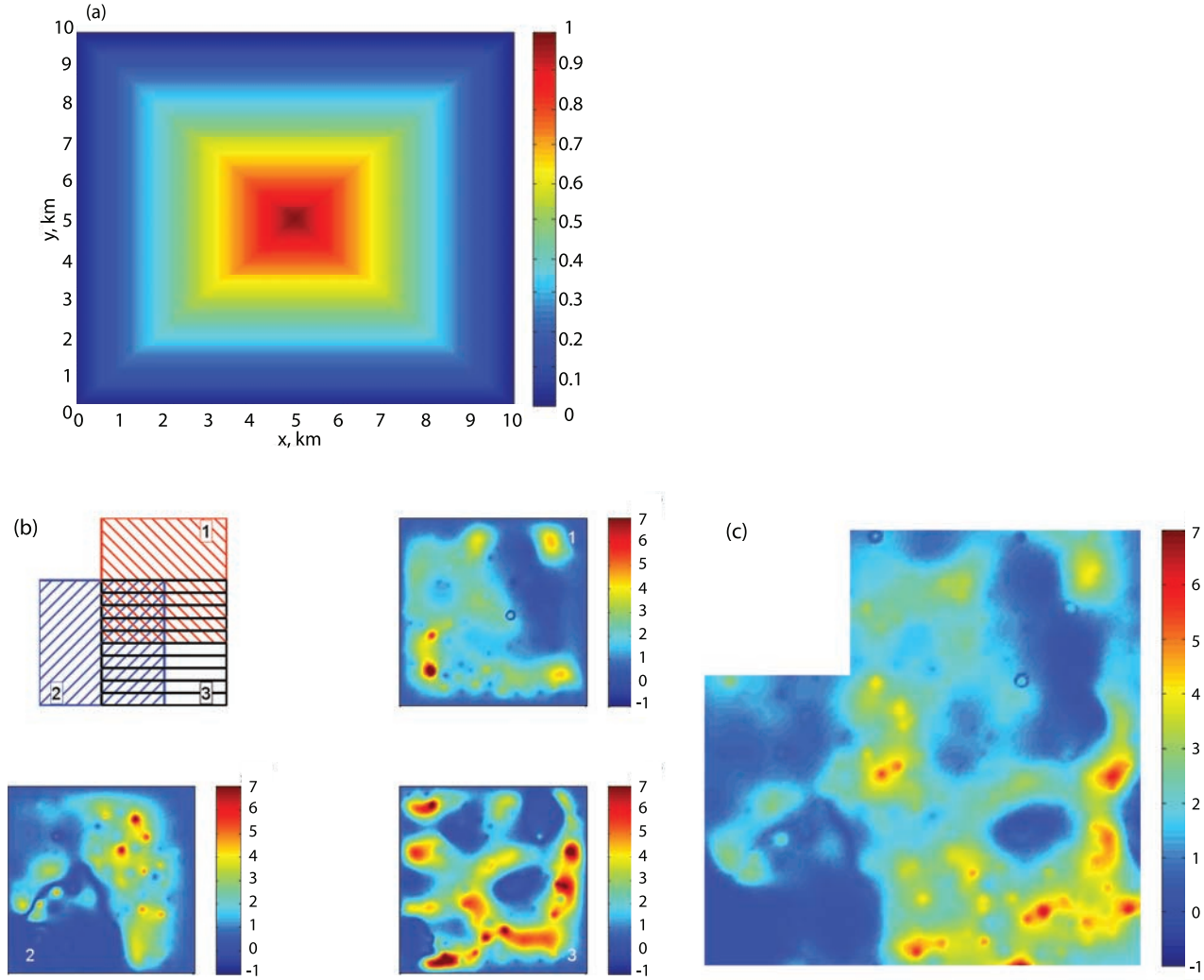

Figure 4. (a) Weight function used for β averaging; (b) example of overlaying blocks and β, 10^5 (Pa s $m^{-1})^{\frac{1}{2}}$ inverted for each block; and (c) weighted averaged $\beta \times 10^{-5}$ over the same area shown in Figure 4b.

areas with larger β (and τ), "sticky spots," but the upstream most such zone displayed in Figure 2c has a larger number of these spots. Figure 6 shows a distinctive ridge of strong basal traction that outlines the west boundary of the upstream fast-flow zone (Figure 2c). As could be seen from Figures 5a and 6 (southeast part of the domain), a small basal friction coefficient and low basal shear in an isolated point is not a sufficient condition for locally fast flow. It seems that large areas with low β and small numbers of sticky spots tend to result in ice flow that is faster than otherwise, however this is not always the case. These results emphasize the nonlocal character of ice stream flow. In contrast to parts of the ice sheet that are dominated by vertical shear deformation, where ice flow is mostly determined locally, ice stream flow at a particular point in an ice stream strongly depends on surrounding conditions [see, e.g., *Raymond*, 1996]. Interestingly, there is a sticky spot at the mouth of the BIS ($\tau \approx 30$ kPa), but the ice velocity is maximum over this spot.

[15] Stress balance analysis reveals a striking difference between the upstream and the downstream parts of BIS (Figure 7). Driving stress (Figure 7a) is $\sim$3–5 times lower downstream than upstream. Residual stress, which is difference between driving stress and basal shear stress τ, is primarily determined by the driving stress, because it is generally larger than τ over the whole domain (Figures 6 and 7a). As can be seen in MODIS image (Figure 1), the ice surface in the downstream part is much smoother than in the upstream part. All these factors, small driving stress, almost neglectable basal shear, and smoother surface, suggest that ice flow in this area is very similar to ice shelf flow, i.e., ice is virtually afloat (the ice is still aground). A possible explanation for this phenomena could be high saturation of underlying till with subglacial water, and high water pressure. The downstream part of BIS is confined by interstream ridges on each side where ice is most likely frozen to the bed (Figure 1). Subglacial water from the upstream region is forced into a narrow, channel-like, downstream part, resulting in increased water saturation and water pressure, and consequently, very weak basal traction. This also might provide an explanation of the strong tidal modulation

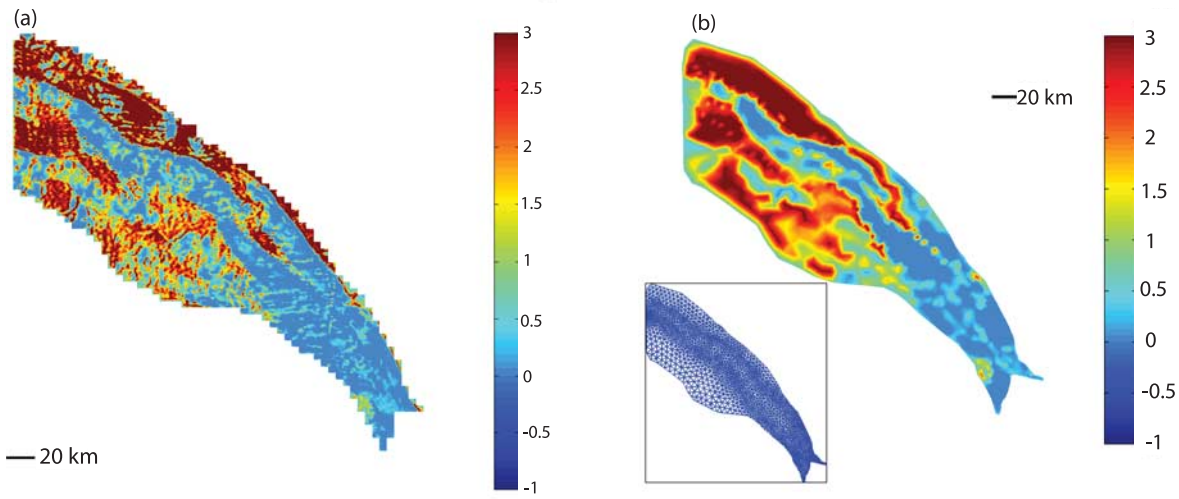

Figure 5. Inverted basal friction coefficients β, 10^5 (Pa s m^{-1})$^{\frac{1}{2}}$. (a) Block-wise inversion and (b) whole domain inversion, inset shows finite element mesh used for that inversion. Both fields have similar patterns, but block-wise inversion reveals large small-scale variations unable to be resolved by whole domain inversion.

of ice flow observed in mouth of BIS [*Anandakrishnan et al.*, 2003].

4. Error and Sensitivity Analysis

[16] Figures 8a and 8b show the misfit between the observed ice speed and the ice speed calculated with β resulting from the block-wise inversion (Figure 8a) and whole domain inversion (Figure 8b). In both cases, patterns of misfit are similar to the observation errors (Figure 2d): larger errors ($\sim$30 m a^{-1}) at transitions between zones of fast and slow flow (lateral boundaries of zones I and II Figure 2c), and smaller errors ($\sim$0–4 m a^{-1}) within zones I and II. Large misfit between calculated and observed velocities at ice flow transitions is equally attributed to two sources: large observation errors and simplifications of the forward model used in the inversion. Vertical shear stresses neglected in the forward model might become important at the lateral boundaries of zones I and II. This result suggests that two approaches can be used to improve large misfit in future efforts: ice velocity observation techniques should be improved over ice flow transitions, and inversion techniques with a full stress balance model should be developed.

[17] As described earlier, ice thickness has the largest errors in measurements (±11 m). We investigate sensitivity of inversion results to this error with the whole domain inversion because the block-wise inversion is too computationally intensive for sensitivity studies of this nature. Also, we expect that spatial patterns of the error will be similar for the whole domain and block-wise inversions, and that results of the whole domain inversion will have higher magnitudes, thus providing an upper bound for estimating the effect of ice thickness uncertainty. A randomly distributed 11 m error was introduced into the ice thickness field, and basal friction coefficients were obtained with this distorted ice thickness. The difference between the two β fields (with and without the introduced ice thickness error) is shown in Figure 8c. Similar to the misfit pattern (Figure 8b), largest sensitivity to thickness error (denoted by larger differences between the two beta fields) tends to be located in the ice flow transitions. Deviations in the ice velocity field caused by both variations in β and errors in ice thickness do not exceed the ice velocity observation errors (Figure 8d).

5. Regression Models

[18] There is a wide range of glaciological problems that require knowledge of ice stream behavior on a large scale without a need to understand the ice stream dynamics in detail. A simple, statistical treatment of ice stream flow would be very useful to such large-scale glaciological problems. In this study, we explore the possibility of establishing simple parameterizations of ice stream flow by developing a relationship between ice stream velocity and various parameters: ice thickness, surface elevation, and basal roughness conditions indicative of where basal friction may be high, on

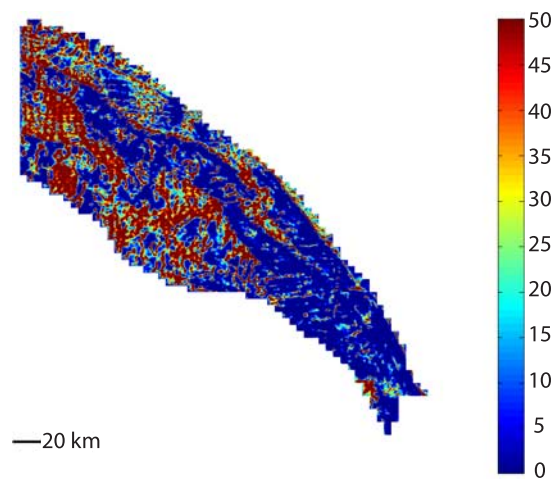

Figure 6. Basal shear (kPa), calculated using equations (4) and (5) and block wise inverted β shown in Figure 5a. Basal shear in zones of fast flowing ice (zones I and II in Figure 2c) is very low $\sim$0.3–3 kPa.

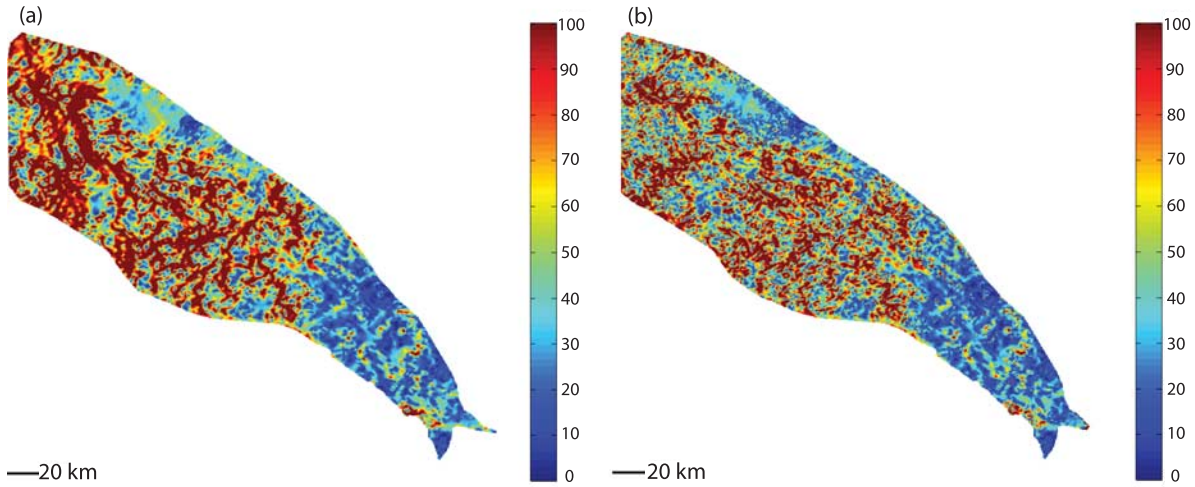

Figure 7. Stresses in ice (kPa) (a) driving stress and (b) residual stress. The difference between driving stress and basal shear shown in Figure 6. Both driving and residual stresses in downstream part of BIS are low magnitude (~10–20 kPa).

the basis of the results of section 4. To describe the "nonlocal" effect mentioned above, we introduce a parameter D defined as the distance to the nearest "high-friction zone," where a high-friction zone is defined as a location where $\beta > 2 \times 10^5$ (Pa s m^{-1})$^{\frac{1}{2}}$. These locations include the lateral confining boundaries of the ice stream and localized sticky spots that can be interspersed in the center of the flow. The choice of the β threshold used in this definition is arbitrary, on the basis of the sharp transition between zones of fast and slow flow in the BIS. This threshold may be specific to this ice stream and should be adopted carefully in application to other fast-flow regions. High-friction zones represent any location where β exceeds a threshold, including areas of very slow or nonmoving ice, e.g., the ice stream margins.

[19] In contrast to inland ice sheet flow, which features vertical shear deformation driven by surface slope, ice stream flow is more ice-shelf-like, and thus, depends more on forces at lateral and frontal boundaries than on the local driving stress determined by local surface slope (Figure S1a of the auxiliary material).[1] This effect is borne out in the velocity data for the BIS, where correlation between ice velocity and the ice thickness gradient and surface elevation gradient are low (−0.3 and −0.1, respectively). Because of this observational fact, the ice thickness and surface elevation gradients were excluded from the regression analysis. Correlations between ice velocity and parameters included in the regression models are: ice thickness −0.5, surface elevation −0.68, basal friction coefficients −0.47, distance to nearest high-friction zone 0.8.

5.1. Linear Regression Model

[20] First, we explore the possibility of a linear relationship between ice velocity and other parameters given by the following regression equation,

$$U = c + hH^k + sS^l + dD^m + f\beta^p, \tag{6}$$

where U is the ice velocity magnitude, c, h, s, d, f are scalar regression coefficients and k, l, m, p are regression exponents. With variable regression exponents we add an extra degree of freedom to the model. It is solved using the Matlab®Optimization Toolbox function "lsqcurvefit" that solves nonlinear data-fitting problems in least squares sense (www.mathworks.com/access/helpdesk/help/toolbox/optim/ug/lsqcurvefit.html).

[21] The coefficients obtained for data and the β field associated with BIS are presented in Table 1, and the velocity field calculated using equation (6) is shown in Figure 9a. Although, the velocity field obtained with the regression model does not exactly resemble the observed field, it captures the most important features: the fast flowing downstream region and the fast-flowing zone upstream (similar to zones I and II in Figure 2c). The explained variance of this regression model is R^2 = 82%, where

$$R^2 = \left(1 - \frac{\sum |U_{\text{regr}} - U_{\text{obs}}|^2}{\sum |U_{\text{obs}} - \bar{U}_{\text{obs}}|^2}\right) 100\%, \tag{7}$$

and U_{regr} is the regressed speed calculated using equation (6), U_{obs} is the observed speed and $\bar{U}_{\text{obs}}$ is the areal mean value of observed speed. Analysis of regression exponents and coefficients of this model show that the model reflects relatively weak dependance of velocity on the ice thickness H and the basal friction coefficient β. Regression exponents involved in treating these parameters, k and p, respectively, are very small, ~0.1. A much stronger dependance is found with the distance to the nearest high-friction zone ($m \sim 0.6$). This emphasizes the importance of nonlocal effects mentioned earlier. The regression parameters of a reduced regression model, where only surface elevation and distance to the nearest high-friction zone are taken into account are shown in parentheses in Table 1. The regression velocity field obtained with this reduced model is very similar to one shown in Figure 9a, and variance of this model is also high (R^2 = 78.2%). A relatively strong dependence of the regressed velocity on the ice surface elevation might be

[1]Auxiliary materials are available in the HTML. doi:10.1029/2008JF001004.

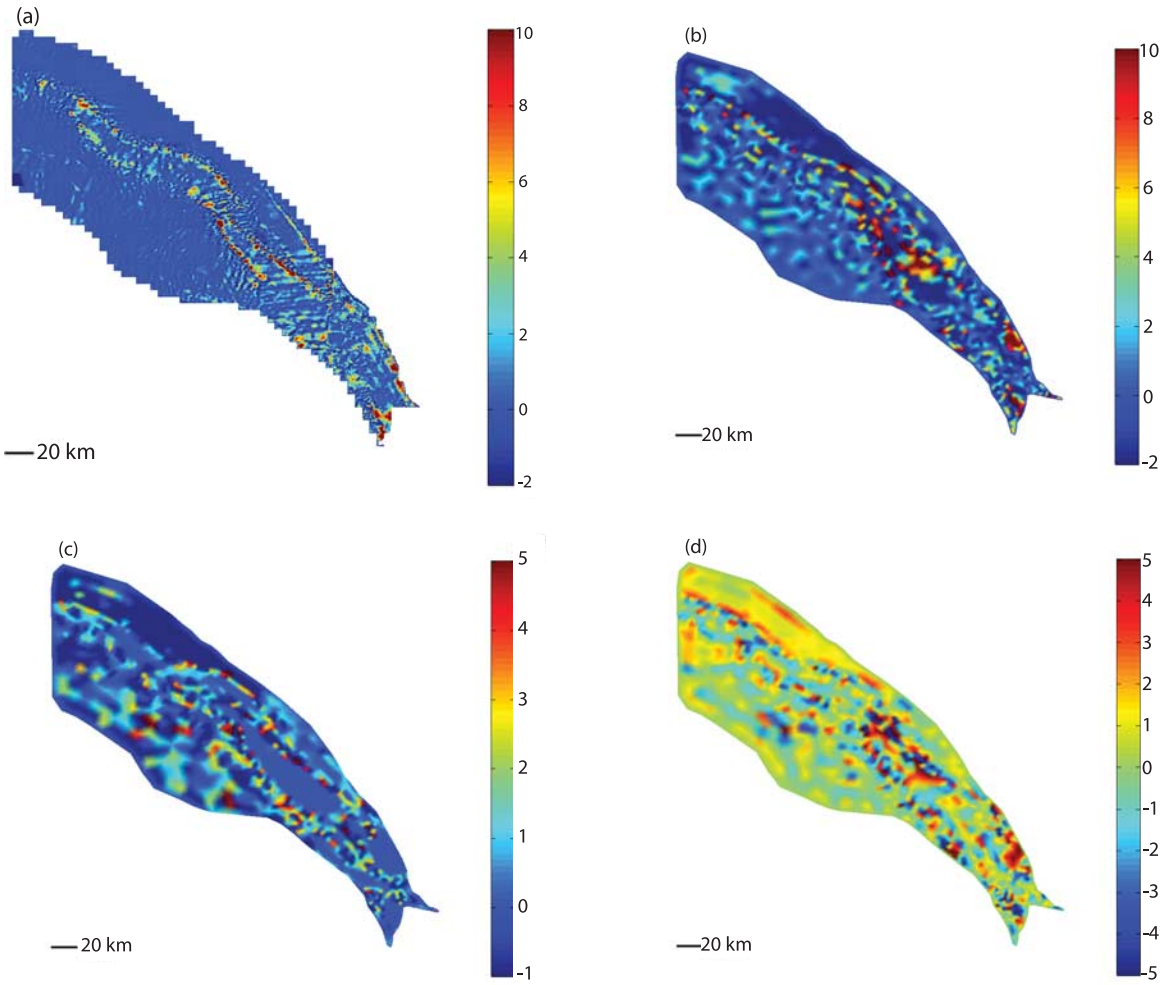

Figure 8. (a) Misfit between observed and calculated velocities in block-wise inversion (m a^{-1}); (b) misfit between observed and calculated velocities in whole domain inversion (m a^{-1}); (c) variations in β caused by 11 m randomly distributed error in ice thickness, 10^4 (Pa s $m^{-1})^{\frac{1}{2}}$; and (d) variations in ice velocity caused by 11 m randomly distributed error in ice thickness and variations in β caused by the same error (m a^{-1}).

associated with a specifics of the BIS stress balance described above: a delicate balance of compressive and tensile forces up and downstream of the BIS determines its concave shape and and velocity field.

[22] As seen in the observed surface velocity (Figure 2c), there are distinctive areas where velocities have specific ranges of values (e.g., less than 100 m a^{-1} or larger than 500 m a^{-1}). It is reasonable to assume that regression parameters could be different for these different velocity ranges. Therefore, we construct a more complex regression model where equation (6) is solved separately for ice velocities that fall in specific ranges. The key improvement of this approach is that the parameter exponents and coefficients are allowed to vary between regions of the ice stream falling in separate velocity ranges. We distinguish four ranges: less than 100, 100–300, 300–500, and larger than 500 m a^{-1}. Results of the regression analysis with the above velocity ranges are shown in Figure 9b and in Table 2. The velocity field calculated using this four-range regression model captures the observed patterns very well, and explains 96% of variability in measured velocity field. Analysis of the regression coefficients and exponents (Table 2) shows results that have some commonality with the whole range regression model where one set of parameter values was applied regardless of velocity: weak dependance on the ice thickness; however, the regression using multiple velocity ranges implies a stronger dependence on the basal friction coefficient β. In practice such a multirange velocity calculation could be implemented in following fashion. Velocities could be calculated using whole range regression coefficients, and then recalculated again using four-range regression coefficients.

5.2. Logarithmic Regression Model

[23] In our second regression model we explore a multiplicative relationship between ice velocity and other parameters using

$$U = cH^k S^l D^m \beta^p, \tag{8}$$

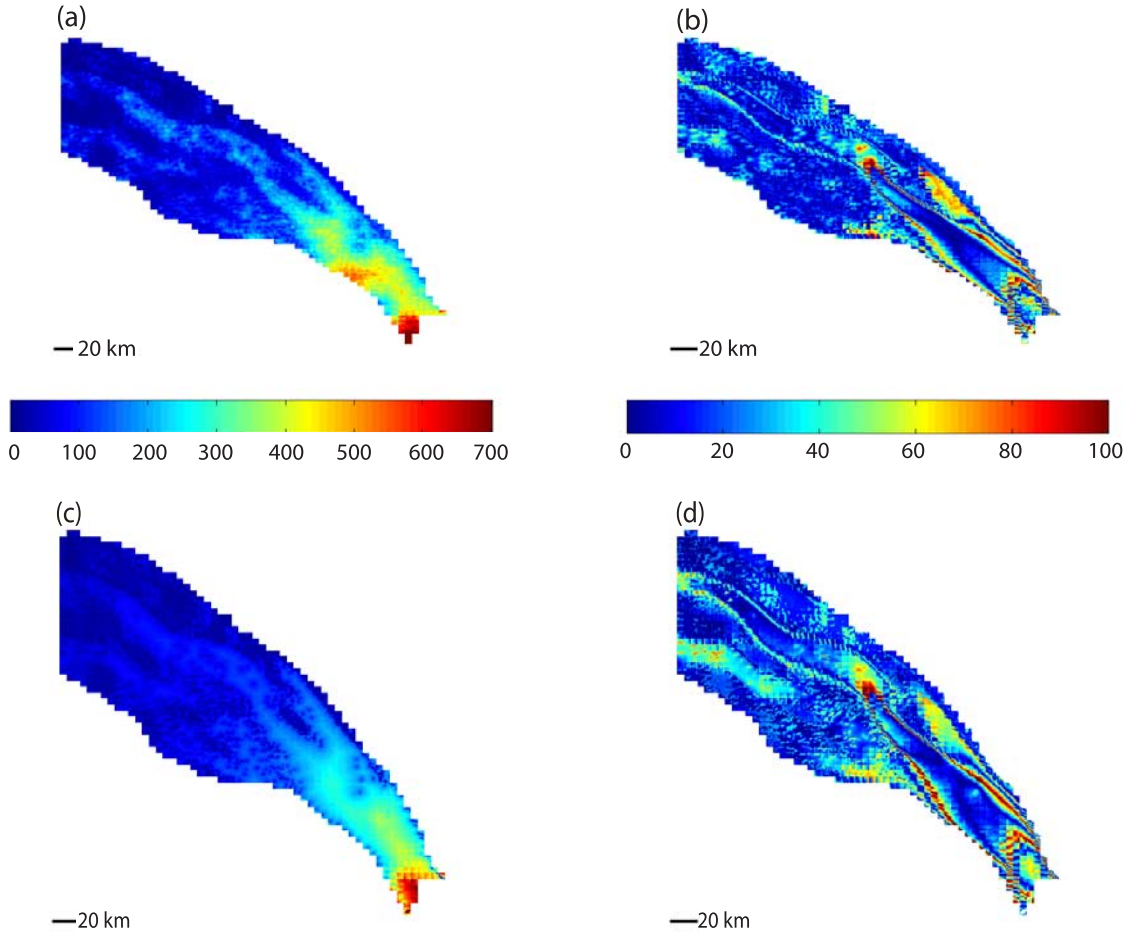

Figure 9. Regression model results. (a) Ice speed (U m a^{-1}) calculated with whole domain linear regression model (R^2 = 82%), (b) speed difference (ΔU m a^{-1}) between observed ice speed and calculated with four-range linear regression model (R^2 = 96%), (c) ice speed (U m a^{-1}) calculated with whole domain logarithmic regression model (R^2 = 74%), and (d) speed difference (ΔU m a^{-1}) between observed ice speed and calculated with four-range logarithmic regression model (R^2 = 95%). Color bars are the same for Figures 9a and 9c and for Figures 9b and 9d.

where parameters and variables are the same as above. Taking the logarithm of both side of equation (8), the equation is converted into a linear regression problem where exponents k, l, m and p, appear as coefficients of a linear relation. That ice flow speed is dependent on H, S, D and β, in the form expressed by equation (8) is similar to one argued by *Raymond* [1996] in his analysis of shear margins and how basal conditions affect ice stream flow. According to his study, where it is assumed that basal conditions are uniform along the flow and variable only across the flow, ice velocity is proportional to a product of power functions of ice thickness, distance to the lateral margins, and difference between driving and basal stresses.

[24] The logarithmic regression model (equation (8)) explains less than 50% of the variance of the observed velocity (R^2 = 41%). Better agreement with observations is achieved when ice thickness, H, and basal friction, β, are eliminated as regression parameters, and only surface elevation, S, and distance to the nearest high-friction zone, D, are taken into account, i.e.,

$$U = cS^l D^m. \tag{9}$$

[25] In this case R^2 = 74%. The regression coefficients and exponents for this second, and best performing, version of the logarithmic regression models are presented in Table 3. The parameterized velocity map is shown in Figure 9c.

[26] As with the linear regression model of the previous section, the logarithmic model is improved if regression parameters are allowed to differ in 4 different ranges of

Table 1. Coefficients and Variance R^2 of the Linear Regression Model Constructed for the Whole Domain[a]

	hH^k		sS^l		dD^m		$f\beta^p$		
c	h	k	s	l	d	m	f	p	R^2
−408(−61.95)	0.05	−0.03	2.05×10^4(8985)	−0.88(−0.7)	0.1(1.65)	0.78(0.65)	537	−0.03	82%(78.2%)

[a]Numbers in parenthesis are coefficients of a reduced model, included surface elevation S and distance to a high-friction zone D.

Table 2. Coefficients and R^2 of the Linear Regression Model Constructed for Four Different Velocity Ranges[a]

		hH^k		sS^l		dD^m		$f\beta^p$		
Velocity Range	c	h	k	s	l	d	m	f	p	R^2
<100 m a^{-1}	−237.76(−27.8)	130.55	0.12	−13.34(197.7)	0.33(−0.2)	0.19(0.76)	0.68(0.51)	-3.7×10^{-4}	0.82	96%(95%)
100–300 m a^{-1}	−148.98(149.96)	−0.49	0.6	154.4(−0.14)	−0.37(0.79)	0.32(0.23)	0.59(0.63)	132.16	−0.2	96%(95%)
300–500 m a^{-1}	262.92(504.9)	-6.8×10^{-3}	0.6	613.5(−10.57)	−0.27(0.46)	$0.78(3.1 \times 10^{-3})$	0.28(0.66)	-1.3×10^{-5}	0.7	96%(95%)
>500 m a^{-1}	604(727.57)	−389	0.03	−4.22(−32.1)	0.58(0.3)	0.67(0.13)	0.35(0.45)	0.25	0.5	96%(95%)

[a]Numbers in parenthesis are coefficients of a reduced model, including surface elevation S and distance to a high-friction zone D.

velocities. Parameterized ice velocity resulting from the regression expressed by equation (9) for the same 4 velocity ranges used in the previous linear regression model, explains 95% of measured speed variance. Table 3 presents the corresponding coefficients and exponents, and Figure 9d shows the difference between observed and calculated ice velocity magnitudes.

6. Summary and Conclusions

[27] The block-wise inversion methodology for converting surface observations into ice stream basal conditions developed here has both conceptual and computational advantages. Conceptually, it accounts for observed data better than the whole domain inversion, because it introduces additional internal boundaries where observed velocities are prescribed. These prescriptions impose greater fidelity to observed velocity in the small-scale interiors of the blocks. With the development of better higher-order ice stream models, spatial resolution limitations should disappear and block resolution should be determined by data resolution and computational capacities. This offers the prospect of allowing for reconstruction of the ice stream basal conditions in fine scale, and would contribute to a better understanding of ice stream dynamics. The block-wise inversion could be used as a standard methodology for a systematic inversion of Antarctic ice stream basal conditions. Such a standardized approach would be very useful in ice stream studies because it would provide uniform spatial resolution of output results. The block-wise inversion procedure also provides many computational advantages, the most important of which is that matrix factorization required in the process is significantly easier than in the whole domain inversion. The block-wise inversion approach is also amenable to implementation on a parallel multiple processer computing platform.

[28] An application of block-wise inversion to BIS reveals a complex structure in the basal friction coefficient field. In both fast-flowing regions (zones I and II in Figure 2c) basal friction coefficients, β, are small, and in both regions there are areas with much larger β (sticky spots). The upstream zone (I) has "stronger" sticky spots (β is significantly larger) than in the downstream zone (II). The driving stress and the basal shear stress calculated from basal friction coefficients resulting from the inversion are significantly lower in this zone than elsewhere. This result might imply the presence of very weak basal till that is highly saturated with water under zone II. This result has been independently suggested by analysis seeking explanation of the tidally modulated flow on the ice stream [*Anandakrishnan et al.*, 2003]. Both the basal friction coefficient and the basal shear stress resulting from the data inversion illustrate the nonlocal character of ice stream flow. Despite the presence of sticky spots in fast flowing zones, ice does not necessarily slow. Moreover, despite "slippery spots" (areas with much lower β) in strong traction domains, ice does not necessarily accelerate.

Table 3. Coefficients and R^2 of the Logarithmic Regression Model Constructed for the Whole Domain and Different Velocity Ranges[a]

Velocity Range	c	$S^l\ l$	$D^m\ m$	R^2
Whole domain	4715	−0.87	0.22	74%
<100 m a^{-1}	120	−0.3	0.15	95%
100–300 m a^{-1}	220.4	−0.11	0.06	95%
300–500 m a^{-1}	568	−0.16	0.05	95%
>500 m a^{-1}	599	−0.08	0.04	95%

[a]Logarithmic regression model shown by equation (9).

[29] Spatial patterns of the misfit between observed velocities and velocities calculated using inverted basal friction coefficients are similar to the ice velocity observation errors. Large errors and misfits are along the margins of fast-flowing zones. The possible reasons for large misfits at those locations are large observation errors and simplifications inherent in the ice flow model used for the inversion procedure. Better ice velocity observation techniques and better ice flow models are required to identify the primary reason of the misfit patterns. As a sensitivity test shows, misfits in the inverted basal friction coefficients caused by randomly distributed error in the ice thickness field and in the ice velocity fields calculated with these coefficient have patterns somewhat similar to misfit between observed and calculated velocities, i.e., larger values along the margins and at the locations of high-friction zones. Magnitudes of the velocity differences due to ice thickness error are less then the ice velocity observation errors.

[30] In the second part of this study, we explored the construction of several regression models that would be useful as parameterizations of ice stream flow in larger-scale models. The regression variables to which the ice stream flow was assumed to depend include: ice thickness, surface elevation, basal friction coefficient and distance to nearest high-friction zone ($\beta > 2 \times 10^5$(Pa s m^{-1})$^{\frac{1}{2}}$). As our results show, a linear regression model constructed for the whole domain can capture major patterns of observed ice velocity, and explain 82% of the observed velocity variability. A weak dependance of the regressed velocity on ice thickness and basal friction coefficients suggests that a relatively good estimate of ice velocity could be achieved from surface elevation and distances to nearest high-friction zones alone. In contrast to surface elevation, locations of high friction (needed to prescribe distance to nearest high-friction zones) is not directly measured at the present time. Bed roughness [*Bingham and Siegert*, 2007] or various roughness features visible in surface imagery, e.g., using MODIS images, could perhaps be used as a proxy for estimating the location of

high-friction zones [*MacAyeal et al.*, 1995]. This offers the prospect of allowing for reconstruction of the ice stream basal conditions in fine scale, which subsequently contributes to a better understanding of ice stream dynamics.

[31] Better performing parameterizations of ice stream flow can be obtained if the linear regression model is modified to allow parameters to vary within subdomains defined by ranges of velocities. With this approach, the regressed velocity field explains 96% variability of the observed field. A reduced regression model that uses only surface elevation and distance to the nearest high-friction zone produces good results as well (its R^2 is 94%). Dependence of these simple parameterizations, both for the whole domain and for subdomain regression approaches, is primarily on distance to the nearest high-friction zone rather than on other basal conditions.

[32] In the case of the logarithmic regression model, the best agreement with observations is achieved if only two parameters are taken into account: surface elevation and distance to nearest high-friction zone (R^2 = 74%). As in the case with the linear regression model, application of the logarithmic model for subdomains where velocities fall in specific ranges significantly increases agreement with observations (R^2 = 95%). The improved performance of the linear regression model relative to the logarithmic model that has a physical justification in the analysis of idealized ice streams that lack longitudinal variations in basal conditions emphasizes the role of along-flow variation of basal conditions.

[33] The proposed regression models are appealing in their simplicity and in their dependence on very few parameters. Since these models were developed for an isolated ice stream (the BIS), universality of their results remains to be determined. One aspect of the regression analysis presented here is that the ice velocity appears to depend relatively little on the gradients of ice thickness and surface elevation. This result may be a special feature of the BIS that may not apply to other ice streams where stiffer basal traction associates with larger, more spatially variable surface elevation and ice thickness gradients. A possible strategy for improving the universality of regression models may include development of similar models for other ice streams, creation of single regression models (linear, logarithmic, or other) using parameters from multiple ice streams, and detailed studies of idealized ice streams. Subdomain regression models are most likely less portable, nevertheless their results might be helpful in determining parameters of a universal regression model that could encompass general behavior of all ice streams. The question of whether regression parameters are time variable is important in context of paleo ice stream studies; and the best, most productive result would be to find temporally and spatially invariant parameters (universal parameters) that simply address the effects of a few time-varying state variables (regression objects).

[34] **Acknowledgments.** We thank the associated editor, Shawn Marshall, Hilmar Gudmundsson, and anonymous reviewer for insightful comments and valuable suggestions that helped to improve the manuscript. O.V.S. was supported by an appointment to the NASA Postdoctoral Program at the Goddard Space Flight Center, administered by Oak Ridge Associated Universities through a contract with NASA, and by NSF grant OPP-0632168. D.R.M.'s participation was supported by NSF OPP-0229546.

References

Alley, R. B., D. D. Blankenship, C. R. Bentley, and S. T. Rooney (1987), Till beneath ice stream B: 3. Till deformation: Evidence and implications, *J. Geophys. Res.*, *92*(B9), 8921–8929.

Anandakrishnan, S., D. Voigt, and R. B. Alley (2003), Ice stream D flow speed is strongly modulated by the tide beneath the Ross Ice Shelf, *Geophys. Res. Lett.*, *30*(7), 1361, doi:10.1029/2002GL016329.

Bentley, C. (1987), Antarctic ice streams: A review, *J. Geophys. Res.*, *92*(B9), 8843–8858.

Bingham, R., and M. Siegert (2007), Radar-derived bed roughness characterization of Institute and Möller ice streams, West Antarctica, and comparison with Siple Coast ice streams, *Geophys. Res. Lett.*, *34*, L21504, doi:10.1029/2007GL031483.

Blankenship, D., C. Bentley, S. Rooney, and R. Alley (1986), Seismic measurements reveal a saturated porous layer beneath an active Antarctic ice stream, *Nature*, *322*(6074), 54–57.

Blankenship, D., D. Morse, C. Finn, R. Bell, M. S. D. Peters, K. S. Hodge, M. Studinger, J. Behrendt, and J. Bronzena (2000), Geologic controls on the initiation of rapid basal motion for West Antarctic Ice Streams: A geophysical perspective including new airborne radar sounding and laser altimetry results, in *The West Antarctic Ice Sheet: Behavior and Environment*, *Ant. Res. Ser.*, vol. 77, edited by R. B. Alley and R. A. Bindschadler, pp. 157–199, AGU, Washington, D. C.

DiMarzio, J., A. Brenner, R. Schutz, C. A. Shuman, and H. J. Zwally (2007), GLAS/ICESat 500 m Laser Altimetry Digital Elevation Model of Antarctica, http://nsidc.org/data/nsidc-0304.html, Natl. Snow and Ice Data Cent., Boulder, Colo.

Hindmarsh, R. C. A. (2004), A numerical comparison of approximations to the Stokes equations used in ice sheet and glacier modeling, *J. Geophys. Res.*, *109*, F01012, doi:10.1029/2003JF000065.

Isakov, V. (1998), *Inverse Problems for Partial Differential Equations*, 1st ed., 284 pp., Springer, New York.

Joughin, I. (2002), Ice-sheet velocity mapping: A combined interferometric and speckle-tracking approach, *Ann. Glaciol.*, *34*(2), 195–201.

Joughin, I., D. MacAyeal, and S. Tulaczyk (2004), Basal shear stress of the Ross ice streams from control method inversions, *J. Geophys. Res.*, *109*, B09405, doi:10.1029/2003JB002960.

MacAyeal, D. R. (1989), Large-scale ice flow over a viscous basal sediment: Theory and application to ice stream B, Antarctica, *J. Geophys. Res.*, *94*(B4), 4071–4087.

MacAyeal, D. R. (1992a), Irregular oscillations of the West Antarctic ice sheet, *Nature*, *359*(6390), 29–32.

MacAyeal, D. R. (1992b), The basal stress-distribution of ice stream E, Antarctica, inferred by control methods, *J. Geophys. Res.*, *97*(B1), 595–603.

MacAyeal, D. R., R. A. Bindschadler, and T. A. Scambos (1995), Basal friction of Ice Stream E, West Antarctica, *J. Glaciol.*, *41*(138), 247–262.

Peters, L. E., S. Anandakrishnan, R. B. Alley, J. P. Winberry, and D. E. Voigt (2006), Subglacial sediments as a control on the onset and location of two Siple Coast ice streams, West Antarctica, *J. Geophys. Res.*, *111*, B01302, doi:10.1029/2005JB003766.

Raymond, C. (1996), Shear margins in glaciers and ice sheets, *J. Glaciol.*, *42*(140), 90–102.

Rose, K. (1979), Characteristics of ice flow in Marie Byrd Land, Antarctica, *J. Glaciol.*, *24*(90), 63–76.

Schoof, C. (2006), A variational approach to ice stream flow, *J. Fluid Mech.*, *556*, 227–251, doi:10.1017/S0022112006009591.

Tulaczyk, S., W. Kamb, and H. Engelhard (2000), Basal mechanics of Ice Stream B, West Antarctica: 1. Till mechanics, *J. Geophys. Res.*, *105*(B1), 463–481.

Vieli, A., and A. Payne (2003), Application of control methods for modelling the flow of Pine Island Glacier, West Antarctica, *Ann. Glaciol.*, *36*(1), 197–204.

R. A. Bindschadler, Hydrospheric and Biospheric Sciences Laboratory, NASA Goddard Space Flight Center, Code 614, Building 33, Room A112, Greenbelt, MD 20771, USA.

D. R. MacAyeal, Department of the Geophysical Sciences, University of Chicago, 5734 South Ellis Avenue, Chicago, IL 60637, USA.

O. V. Sergienko, Geology Department, Portland State University, P.O. Box 751, Portland, OR 97207, USA. (sergienk@pdx.edu)

P. L. Vornberger, Science Applications International Corporation, 4600 Powder Mill Road, Beltsville, MD 20705, USA.